STATE OF THE CLIMATE IN 2020

THE TROPICS

H. J. Diamond and C. J. Schreck, Eds.

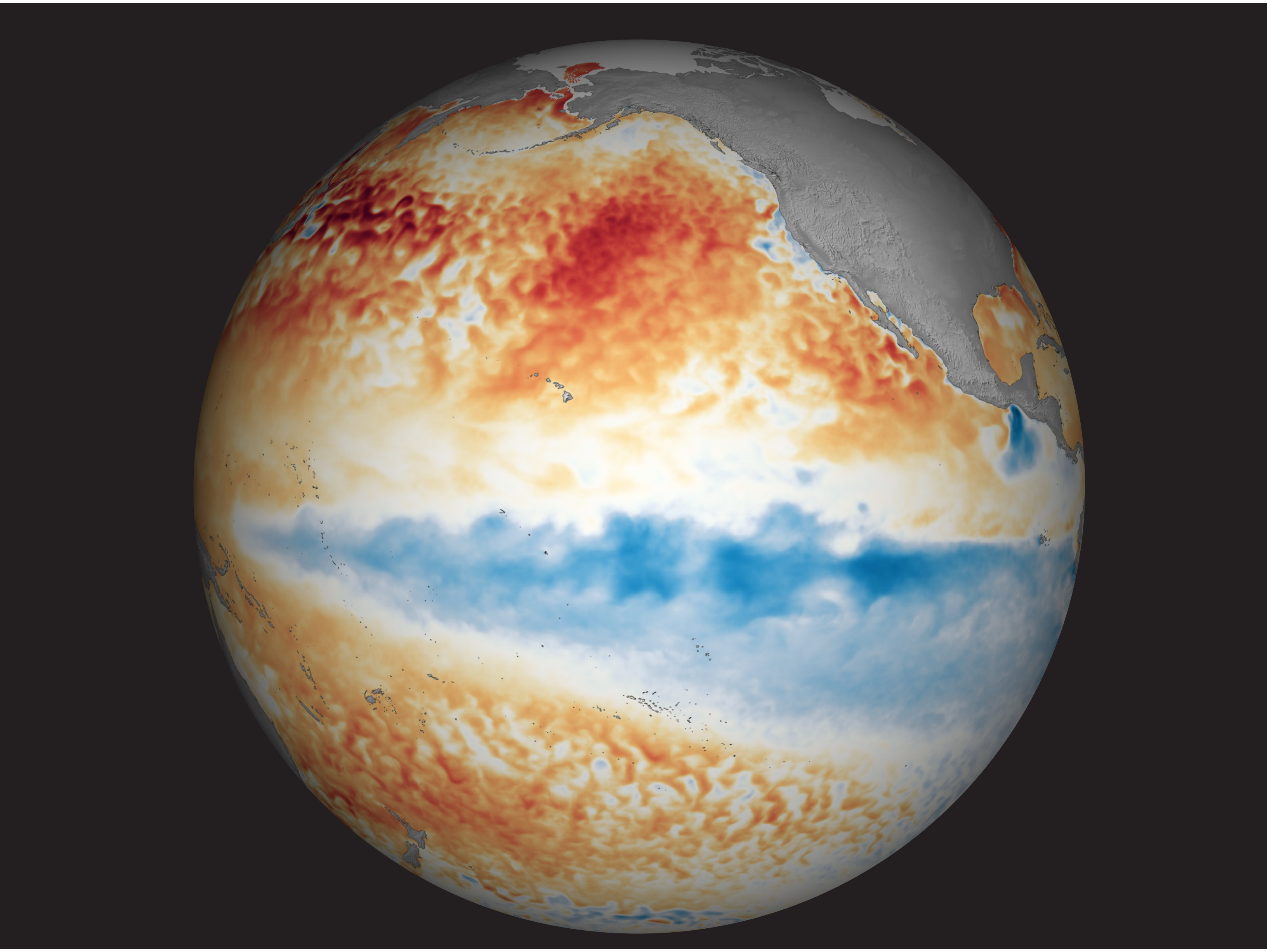

Special Online Supplement to the *Bulletin of the American Meteorological Society* Vol.102, No. 8, August, 2021

https://doi.org/10.1175/BAMS-D-21-0080.1

Corresponding author: Howard J. Diamond / howard.diamond@noaa.gov

©2021 American Meteorological Society
For information regarding reuse of this content and general copyright information, consult the AMS Copyright Policy.

Table 4.2. Global counts of TC activity by basin for 2020. "+" denotes top tercile; "++" is top 10%; "-" is bottom tercile; "--" is bottom 10% (all relative to 1981–2010). "+++" denotes record values for the entire IBTrACS period of record. (Note that some inconsistencies between Table 4.2 and the text of the various basin write-ups in section g exist and are unavoidable, as tallying global TC numbers is challenging and involves more than simply adding up basin totals, because some storms cross TC basin boundaries, some TC basins overlap, and multiple agencies are involved in tracking and categorizing TCs.)

Basin	TCs	HTCs	Major HTCs	SS Cat 5	ACE (× 10^4 kt^2)
North Atlantic	30 +++	14 ++	7 ++	0	180 +
Eastern Pacific	17	4 ––	3	0	77 –
Western Pacific	23 –	12 –	7 –	1	150 ––
North Indian	5 +	4 ++	2 ++	1 ++	27 +
South Indian	11 +	6	3	0	54 –
Australia	10	3 –	0	0	31 –
Southwest Pacific	9	5 +	1	1 ++	56
Global Totals	**102** ++	**48**	**23**	**3**	**574** ––

2) *Atlantic basin*—G. D. Bell, M. Rosencrans, E. S. Blake, C. W. Landsea, H. Wang, S. B. Goldenberg, and R. J. Pasch

(I) 2020 SEASONAL ACTIVITY

The 2020 Atlantic hurricane season produced 30 named storms, of which 14 became hurricanes and seven of those became major hurricanes (Fig. 4.22a). The Hurricane Database 2 (HURDAT2; Landsea and Franklin, 2013) 1981–2010 seasonal averages (included in IBTrACS) are 12.1 named storms, 6.4 hurricanes, and 2.7 major hurricanes (Landsea and Franklin 2013). The 30 named storms during 2020 surpasses the previous record of 28 set in 2005. The 14 hurricanes during 2020 are the second most on record behind 15 observed in 2005, seven major hurricanes tied with 2005 for the most on record.

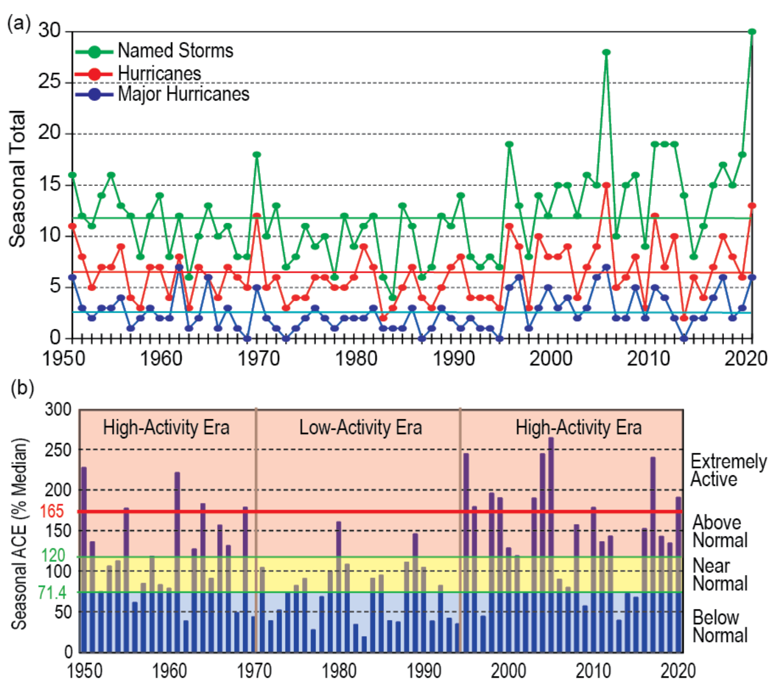

Fig. 4.22. Seasonal North Atlantic hurricane activity during 1950–2020. (a) Numbers of named storms (green), hurricanes (red), and major hurricanes (blue). (b) The ACE index expressed as percent of the 1981–2010 median value. ACE is calculated by summing the squares of the 6-hourly maximum sustained surface wind speed (kt) for all periods while the storm is at least tropical storm strength. Red, yellow, and blue shadings correspond to NOAA's classifications for above-, near-, and below-normal seasons, respectively (http://www.cpc.ncep.noaa.gov/products/outlooks/background_information.shtml). The thick red horizontal line at 165% of the median ACE value denotes NOAA's threshold for an extremely active season. Vertical brown lines separate high- and low-activity eras. Note that there is a low bias in activity during the 1950s to the early 1970s due to the lack of satellite imagery and a technique (Dvorak) to interpret tropical cyclone intensity for systems over the open ocean. (Source: HURDAT2 [Landsea and Franklin 2013].)

Nine of 30 named storms during 2020 were short-lived (≤2 days). There has been a large artificial increase (approximately five per year) in these "shorties" since 2000 (Landsea et al. 2010). These increased counts primarily reflect new observational capabilities such as scatterometers, Advanced Microwave Sounding Units, and the Advanced Dvorak Technique, and have no association with any known climate variability (Villarini et al. 2011).

The 2020 seasonal ACE value (Bell et al. 2000) was 191.5% of the 1981–2010 median (which is 92.4×10^4 kt^2; Fig. 4.22b). This value is the sixth largest since 1970 and is above NOAA's threshold for both an above-normal (120%) and an extremely active (165%) season. There have now been a record five consecutive above-normal seasons, which surpasses the previous record of four set in 1998–2001. Since the current Atlantic high-activity era began in 1995 (Goldenberg et al. 2001; Bell et al. 2019, 2020), there have been 18 above-normal seasons, with 10 being classified as extremely active. By comparison, the preceding 24-year low-activity era of 1971–94 had only two above-normal seasons, and none were extremely active.

(II) STORM FORMATION TIMES, REGIONS, AND LANDFALLS

Substantial TC activity occurred throughout the 2020 hurricane season (Fig. 4.23a). May–July saw a record nine named storms. Seven of those, of which four were "shorties," formed in the extratropics from pre-existing extratropical disturbances. On average, 1–2 named storms form per year during this period.

August–October (ASO), typically the most active part of the hurricane season, featured 18 named storms during 2020, with a record 10 forming in September. Ten of the 18 named storms became hurricanes, and four of those became major hurricanes. Most of these storms (13 of 18) formed in the Main Development Region (MDR, green box in Fig. 4.23c), which is also typical of an above-normal season. The MDR spans the tropical North Atlantic Ocean and Caribbean Sea between 9.5°N and 21.5°N (Goldenberg and Shapiro 1996; Goldenberg et al. 2001; Bell and Chelliah 2006; Bell et al. 2017, 2018, 2019). November 2020 saw three named storms, with two becoming major hurricanes over the western Caribbean Sea and striking Nicaragua as Category 4 storms, and generated the second-most Atlantic ACE on record (36×10^4 kt^2), trailing only 1932 (71×10^4 kt^2). On average, November sees only one named storm every other year. Only five major hurricanes have occurred in November in the previous 70 years (1950–2019), and 2020 had two.

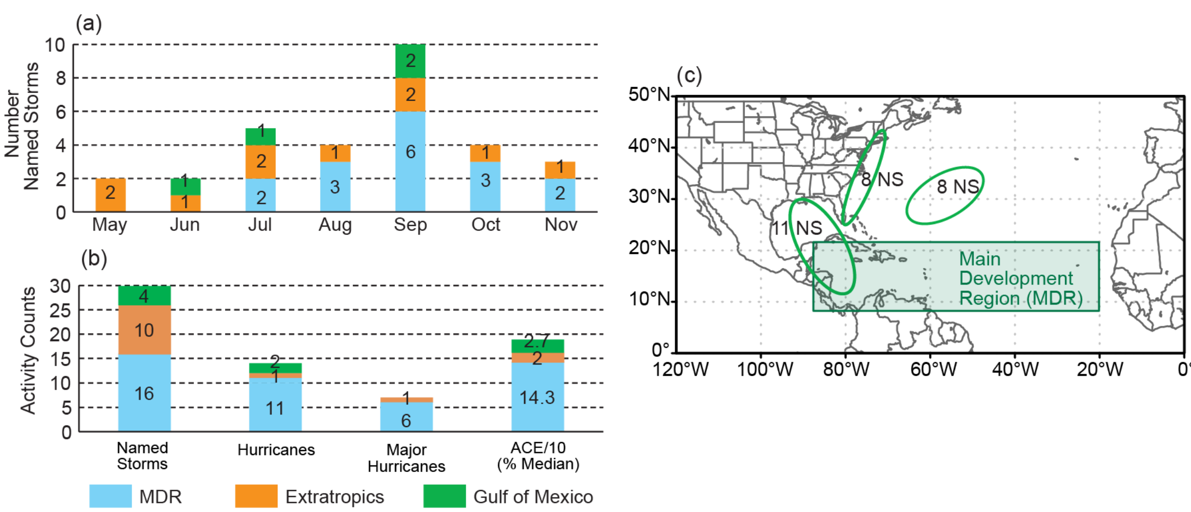

Fig. 4.23. Atlantic TC activity in 2020: (a, b) Storm counts and (c) areas of increased track density. In (a), named storm counts are shown for the month and region the storm was first named. In (b), total seasonal counts for the three storm classifications and ACE are shown for each region where the storm was first named. ACE reflects the entire storm ACE and is attributed to the region in which the storm was first named. Regions in (a, b) are indicated by the color bar below panel (b). In (c), areas of increased track density are shown by green ovals, and the number of named storms that passed through each region are indicated. The Atlantic MDR is shown by the green box. The "extratropics" includes all regions except for the MDR and Gulf of Mexico. (Source: HURDAT2 [Landsea and Franklin 2013].)

Historically, above-normal seasons result from a sharp increase in the number, intensity, and duration of storms that develop in the MDR. During the 2020 season, 16 of the 30 named storms formed in the MDR (Fig. 4.23b) and accounted for 10 of the season's 14 hurricanes and five of the season's seven major hurricanes. The associated MDR-related ACE value was 143% of the median and far exceeds the ACE of 27% associated with storms first named over the Gulf of Mexico and 20% for storms from the extratropics. This MDR-related ACE value was comparable to the 1981–2010 MDR average for above-normal seasons of 155% of the median. These values are roughly 10 times higher than the MDR average of 15.8% for below-normal seasons (Bell et al 2011).

The actual storm tracks during 2020 (not shown) showed three main regions of exceptionally high track density (Fig. 4.23c). One region extended from the western Caribbean Sea to the central U.S. Gulf Coast experiencing 11 named storms with nine as hurricanes and four of those as major hurricanes. Another region extended along the U.S. Atlantic Coast, with eight named storms, one of which became a hurricane. A third region covered the west-central North Atlantic, also with eight named storms, three of which became hurricanes and two of those became major hurricanes.

The season's storm tracks resulted in a record 12 landfalling storms in the continental United States. Six struck as hurricanes, including five as Category 1–2 storms and one as a Category 4 major hurricane (Hurricane Laura in Louisiana). Regionally, nine named storms (including four Category 1–2 hurricanes and Hurricane Laura) made landfall along the Gulf Coast. Louisiana alone experienced a record five landfalling storms, with two striking as Category 1–2 hurricanes (Delta and Zeta) and Category 4 Hurricane Laura. The U.S Atlantic Coast experienced three landfalling storms, including Category 1 Hurricane Isaias. Elsewhere, two hurricanes (Delta and Zeta) made landfall in Mexico, two major hurricanes (Eta and Iota) made landfall in Nicaragua, and one hurricane (Nana) made landfall in Belize.

(III) SEA SURFACE TEMPERATURES

Four main sea surface temperature (SST) signals were present during ASO 2020 (Fig. 4.24). First, SSTs were above average throughout the MDR (Fig. 4.24a), and the area-averaged SST anomaly was +0.6°C (Fig. 4.24b). The largest anomalies were observed throughout the Caribbean Sea and ranged from +0.5° to +1.0°C. Second, the area-averaged SST anomaly in the MDR was also higher (by 0.35°C) than that of the remainder of the global tropics (Fig. 4.24c). This signal typifies the warm phase of the Atlantic Multi-decadal Oscillation (AMO; Enfield and Mestas-Nuñez 1999; Bell and Chelliah 2006) and is a ubiquitous characteristic of Atlantic high-activity eras such as 1950–70 and 1995–present (Goldenberg et al. 2001; Vecchi and Soden 2007; Bell et al. 2018).

The third SST signal during ASO 2020 reflected above-average temperatures across most of the North Atlantic Ocean. Outside of the MDR, the largest anomalies (exceeding +1.5°C) occupied the western and portions of the central North Atlantic (Fig. 4.24a), where numerous tropical storms and hurricanes tracked across this region. The area-averaged SST anomaly in the western North Atlantic (red box, Fig. 4.24a) was +0.91°C and reflected a continuation of exceptional warmth that began in 2014 (Fig. 4.24d).

The fourth SST signal during ASO 2020 was the development of La Niña (section 4b). As discussed below, La Niña contributed to the extensive hurricane activity from September onward.

(IV) ATMOSPHERIC CONDITIONS

Climatologically, the ASO peak in Atlantic hurricane activity largely reflects the June–September peak in the West African monsoon. The inter-related circulation features of an enhanced monsoon increase hurricane activity, while those of an anomalously weak monsoon suppress it (Gray 1990; Hastenrath 1990; Landsea et al. 1992; Bell and Chelliah 2006; Bell et al. 2018, 2020). The association on multi-decadal time scales between the AMO and Atlantic hurricane activity largely exists because of their common relationship with the West African monsoon (Bell and Chelliah 2006).

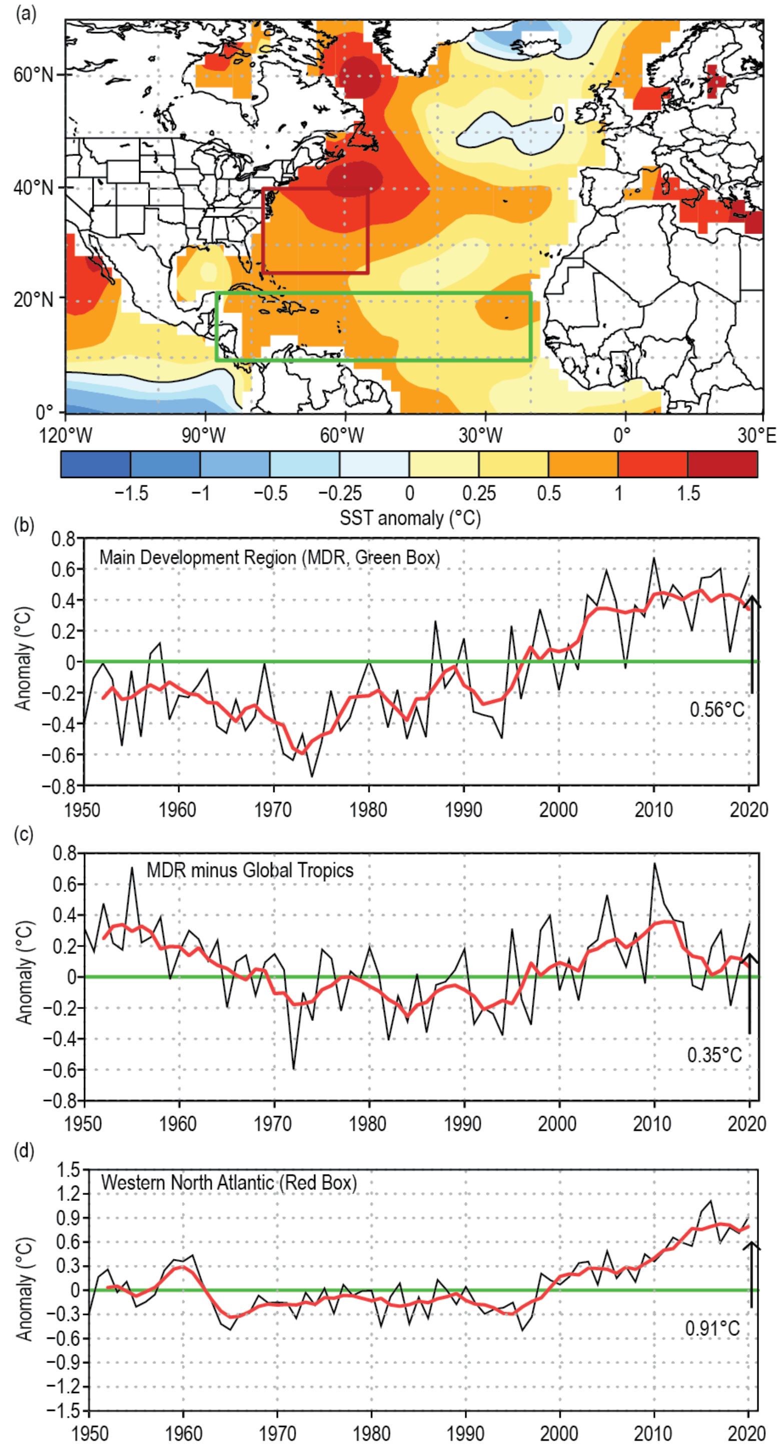

Fig. 4.24. (a) Aug–Oct 2020 SST anomalies (°C). (b)–(d) Time series of Aug–Oct area-averaged SST anomalies (black) and 5-point running mean of the time series (red), (b) in the MDR (green box in (a) spanning 20°–87.5°W and 9.5°–21.5°N), (c) difference between the MDR and the global tropics (20°S–20°N), and (d) in the western North Atlantic (red box in (a) spanning 55°–77.5°W and 25°–40°N). Anomalies are departures from the 1981–2010 period means. (Source: ERSST-v5 [Huang et al. 2017].)

The West African monsoon was enhanced during July–September 2020, as indicated by negative outgoing longwave radiation (OLR) anomalies across the African Sahel (red box, Fig. 4.25a). Total OLR values in this region averaged 234 W m^{-2} (Fig. 4.25b), with values less than 240 W m^{-2}, indicating deep tropical convection. Consistent with these conditions, the larger-scale divergent circulation at 200-hPa featured an extensive area of anomalous divergence and a core of negative velocity potential anomalies across subtropical northern Africa (Fig. 4.25c). The OLR time series shows that an enhanced monsoon has largely prevailed throughout the current Atlantic high-activity era and warm AMO of 1995–present (Fig. 4.25b). By contrast, a much weaker monsoon with OLR values well above 240 W m^{-2} in the Sahel region was typical of the low-activity and cool AMO period of the 1980s and early 1990s.

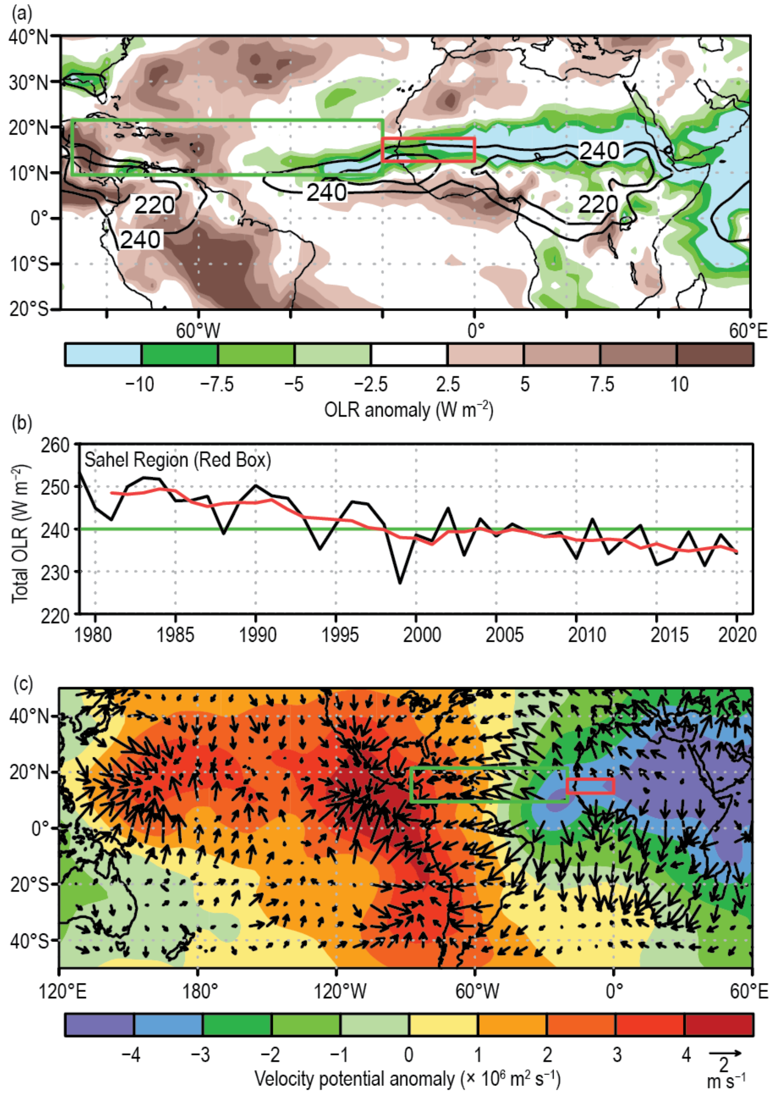

Fig. 4.25. (a) Jul–Sep 2020 anomalous OLR (W m^{-2}), with negative (positive) values indicating enhanced (suppressed) convection. (b) Time series of Jul–Sep total OLR (black) and 5-point running mean of the time series (red) averaged over the African Sahel region (red box in (a), (c) spanning 20°W–0° and 12.5°–17.5°N). (c) Jul–Sep 2020 anomalous 200-hPa velocity potential (× 10^{6} m^{2} s^{-1}) and divergent wind vectors (m s^{-1}). In (a), contours show total OLR values of 220 W m^{-2} and 240 W m^{-2}. In (a), (c), the green box denotes the Atlantic MDR. Anomalies are departures from the 1981–2010 means. (Source: NCEP/NCAR Reanalysis [Kalnay et al. 1996] for velocity potential and wind, and Liebmann and Smith [1996] for OLR.)

During ASO 2020, core atmospheric conditions within the MDR reflected a combination of the enhanced West African monsoon and La Niña. At 200 hPa, one monsoon-related feature was amplified subtropical ridges (indicated by anticyclonic streamfunction anomalies) across the Atlantic Ocean and Africa in both hemispheres (Fig. 4.26a). La Niña impacts in that field (Bell and Chelliah 2006) included cyclonic streamfunction anomalies in both hemispheres of the western and central subtropical Pacific, along with a contribution to the anticyclonic anomalies across the Caribbean Sea and MDR. This combination resulted in a zonal wave-1 anomaly pattern in both hemispheres (green ovals in Fig. 4.26a) that is a classic signal for an extremely active Atlantic hurricane season (Bell and Chelliah 2006; Landsea et al. 1998; Bell et al. 2011).

Within the MDR, this anomaly pattern also reflected a weaker tropical upper-tropospheric trough (indicated by anomalous easterly winds in Fig. 4.26b). Other monsoon-related features were present in the lower troposphere, including lower sea level pressure and weaker easterly and northeasterly trade winds (indicated by westerly and southwesterly anomalies) across the southern half of the central and eastern MDR (Fig. 4.26c).

The resulting combination of anomalous low-level westerlies and upper-level easterlies produced an extensive area of weak vertical wind shear across the tropical Atlantic, western Caribbean Sea, and southern Gulf of Mexico (Figs. 4.27a,b). The area-averaged magnitude of the vertical

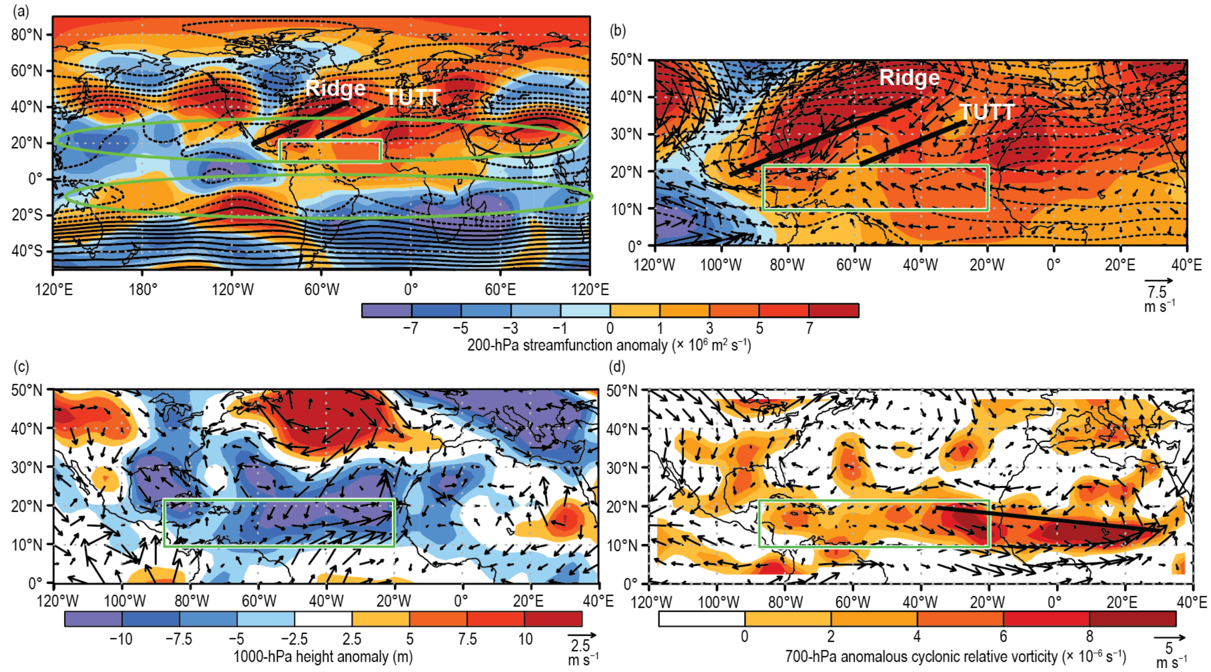

Fig. 4.26. Aug–Oct 2020: (a), (b) 200-hPa streamfunction (contours, interval is 5×10^6 m^2 s^{-1}) and anomalies (shaded), with anomalous vector winds (m s^{-1}) also shown in (b); (c) anomalous 1000-hPa heights (shaded, m) and vector winds; and (d) anomalous 700-hPa cyclonic relative vorticity (shaded, $\times 10^{-6}$ s^{-1}) and vector winds. In (a), (b) the upper-level ridge and TUTT discussed in the text are labeled and denoted by thick black lines. In (a), green ovals highlight the zonal wave-1 pattern discussed in the text. In (d), the thick solid line indicates the axis of the mean African Easterly Jet, which was hand-drawn based on total seasonal wind speeds (not shown). Vector scales differ for each panel and are below right of color bar. The green box denotes the MDR. Anomalies are departures from the 1981–2010 means. (Source: NCEP/NCAR Reanalysis [Kalnay et al. 1996].)

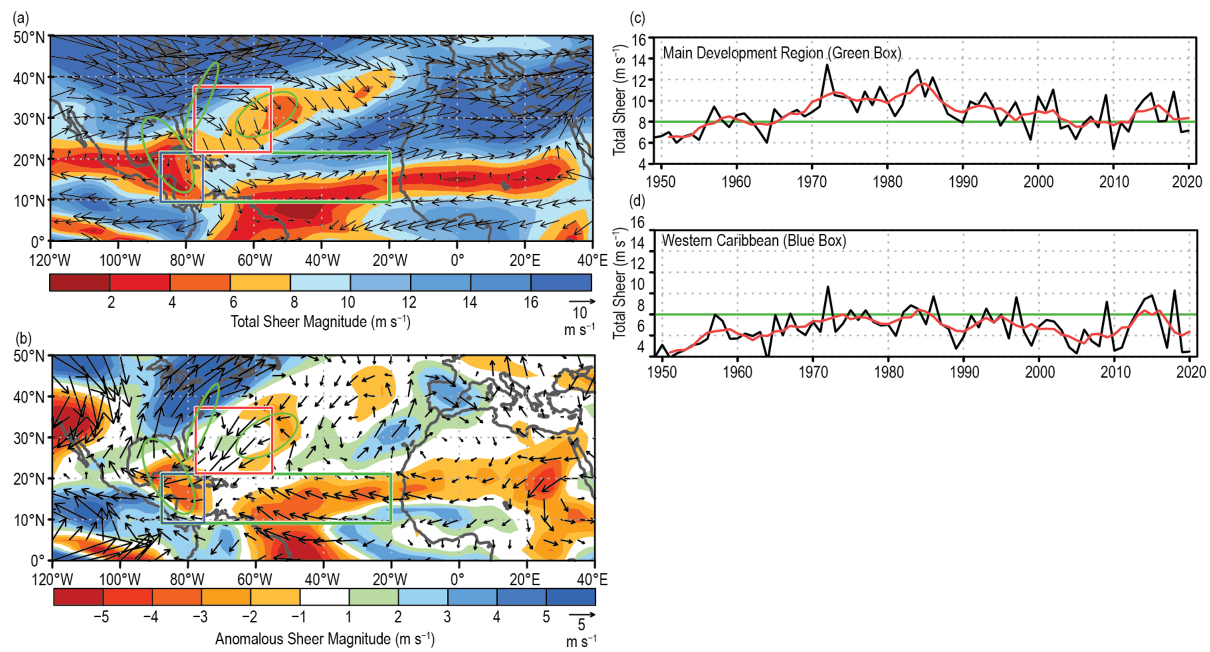

Fig. 4.27. Aug–Oct (ASO) magnitude of the 200–850 hPa vertical wind shear (m s^{-1}): 2020 (a) total magnitude and vector and (b) anomalous magnitude and vector. (c), (d) Time series of ASO vertical shear magnitude (black) and 5-point running mean of the time series (red) averaged over (c) the MDR (green box in (a),(b) spanning 20°–87.5°W and 9.5°–21.5°N), and (d) the western Caribbean Sea (blue box in (a),(b) spanning 87.5°–75°W and 9.5°–21.5°N). Regions with increased track density are shown by green ovals copied from Fig. 4.23c. Anomalies are departures from the 1981–2010 means. (Source: NCEP/NCAR Reanalysis [Kalnay et al. 1996].)

wind shear for the entire MDR was 7.2 m s^{-1} (Fig. 4.27c) and for the western Caribbean Sea was an exceptionally low 4.5 m s^{-1} (Fig. 4.27d). Both of these values are well below the upper threshold of 8 m s^{-1} considered conducive to hurricane formation on monthly time scales (Bell et al. 2017).

The anomalous low-level circulation also reflected an extensive flow of deep tropical moisture into the southern half of the central and eastern MDR. This moisture not only helps feed the monsoon, but also favors increased Atlantic hurricane activity. This situation contrasts with the drier and cooler air that normally accompanies enhanced northeasterly trade winds when the monsoon is weak.

Another aspect of the enhanced West African monsoon system during ASO 2020 was an upward extension of the easterly wind anomalies over the eastern half of the MDR to at least the 700-hPa level (Fig. 4.26d), which is the approximate level of the African Easterly Jet (AEJ). This anomaly pattern contributed to a deep layer of anomalous cyclonic relative vorticity (i.e., increased horizontal cyclonic shear) along the equatorward flank of the AEJ. These conditions are known to favor increased TC activity by helping African easterly waves to be better maintained and by providing an inherent cyclonic rotation to their embedded convective cells (Bell et al. 2004, 2006, 2017, 2018, 2020; Landsea et al. 1998).

The above conditions typified the many above-normal and extremely active seasons seen during the current Atlantic high-activity era; however, interannual signals were also in play during 2020. One of those was La Niña, which supported increased Atlantic hurricane activity over the Caribbean Sea and southern Gulf of Mexico in response to its contribution to weaker vertical wind shear. Another interannual signal was a strong ridge over the western North Atlantic (Figs. 4.26a,b). This ridge contributed to the weak vertical wind shear (Fig. 4.27a), exceptionally warm SSTs over the western North Atlantic (Fig. 4.24d), and to the development of several hurricanes north of the MDR. It also contributed to a highly anomalous steering current (Fig. 4.28), which not only helped focus the storm tracks (Fig. 4.23c), but also contributed to the development of several hurricanes north of the MDR.

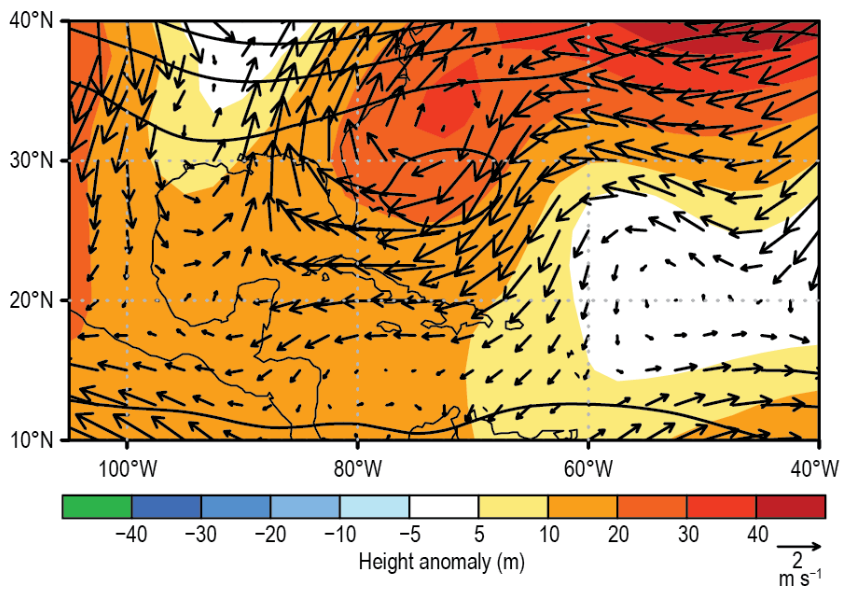

Fig. 4.28. Aug–Oct (ASO) vertically averaged anomalous wind vector between 850 and 200 hPa, along with 500-hPa heights (contours) and anomalies (shaded). (Source: NCEP/NCAR Reanalysis [Kalnay et al. 1996].)

Sidebar 4.1: **Hurricane Laura: A record-setting hurricane for southwest Louisiana—** P. J. KLOTZBACH AND R. E. TRUCHELUT

Fig. SB4.1. GeoColor satellite image of Category 4 Hurricane Laura on 26 Aug at 2050 UTC.

The 2020 Atlantic hurricane season was extremely active, setting the record for most named storms observed in a single season with 30, breaking the old record of 28 set in 2005. The 2020 season also broke the record for most continental United States named storm landfalls in a single season with 11, breaking the old record of nine set in 1916. Of these 11 named storm landfalls, Hurricane Laura was the strongest, making landfall near Cameron, Louisiana, with maximum sustained winds of 130 kt (67 m s^{-1}) on 27 August 2020. Laura caused tremendous damage in Lake Charles and other smaller communities in southwest Louisiana. Laura was the third of four named storms that would make landfall in Louisiana in 2020, tying the old record of four Louisiana named storm landfalls set in 2002.

Here, the meteorological history of Laura will be summarized, along with some of the notable records that the system set. Historical landfall records from 1851–present are taken from the National Hurricane Center/Atlantic Oceanographic and Meteorological Laboratory archive located at: http://www.aoml.noaa.gov/hrd/hurdat/All_U.S._Hurricanes.html. Laura's observed values are taken from Pasch et al. (2021). All times are listed in hours UTC.

Laura became a tropical depression on 20 August in the central tropical Atlantic and slowly intensified to a tropical storm the following day. Westerly shear and dry air entrainment caused persistent displacement of the mid- and low-level circulation centers, and Laura remained a low-end tropical storm as it tracked just south of Puerto Rico on 22 August. Vertical wind shear decreased as Laura crossed the southern portion of the Dominican Republic and Haiti on 23 August. This allowed for better vortex alignment, and maximum sustained winds increased to 55 kt (28 m s^{-1}) before weakening slightly due to both an increase in northerly shear and land interaction with Cuba on 24 August.

Once Laura emerged from the west coast of Cuba, the storm entered a more favorable environment of relatively low wind shear, high sea surface temperatures (~30°C), and increased levels of mid-level moisture. Laura intensified slowly at first, reaching hurricane strength at 1200 UTC on 25 August over the south-central Gulf of Mexico. By early on 26 August, the environment became even more conducive for strengthening, and Laura rapidly intensified from a 75-kt (39-m s^{-1}) Category 1 hurricane at 00 UTC on 26 August to a 130-kt (67-m s^{-1}) Category 4 hurricane at 00 UTC on 27 August (Fig. SB4.1). This 55-kt (28-m s^{-1}) intensification in 24 hours was the fastest intensification rate for an Atlantic named storm in the Gulf of Mexico since Hurricane Karl in 2010, which also intensified by 55 kt (28 m s^{-1}) in 24 hours. Around 6 hours after ending its rapid intensification, Laura made landfall in southwest Louisiana at its peak intensity (i.e., 130 kt [67 m s^{-1}]). Following landfall, Laura rapidly weakened to a tropical storm later on 27 August and then to a tropical depression on 28 August as it tracked north into Arkansas, dissipating early on 29 August over the Ohio Valley.

Fig. SB4.2. Heavily damaged National Weather Service Lake Charles radar following Hurricane Laura. (Image courtesy of Brett Adair, Live Storms Media.)

Hurricane Laura caused tremendous damage in southwestern Louisiana, with a current estimated cost of $19 billion (U.S. dollars). Laura was responsible for seven direct and 34 indirect fatalities in the United States, with 31 additional fatalities occurring in Haiti and nine in the Dominican Republic. About 4 to 6 m of storm surge occurred to the east of Laura's landfall near Creole and Grand Chenier, Louisiana. Lake Charles, Louisiana, suffered extreme wind damage from gusts exceeding 115 kt (59 m s^{-1}), including the destruction of the Lake Charles' Weather Forecast Office's WSR-88D doppler radar (Fig. SB4.2). Laura's track was slightly farther east than anticipated just before landfall, thus sparing Lake Charles a much more significant storm surge.

The 130 kt (67 m s^{-1}) maximum sustained winds at the time of Laura's landfall were the strongest for a Louisiana hurricane since the Last Island Hurricane of 1856 and tied for the fifth strongest on record in the continental United States. Laura's landfall pressure of 939 hPa was the fourth lowest for a Louisiana hurricane on record, trailing Katrina in 2005 (920 hPa), the Last Island Hurricane in 1856 (934 hPa), and Rita in 2005 (937 hPa). Laura also rapidly intensified prior to landfall, defined to be an intensification of ≥30 kt in 24 hours (≥15 m s^{-1} in 24 hours). This was one of three hurricanes in 2020 to rapidly intensify in the 24 hours before its continental U.S. landfall, with the others being Hurricanes Hanna and Zeta. Like Laura, Zeta also rapidly intensified in the 24 hours prior to its landfall in Louisiana. Laura's 40 kt (21 m s^{-1}) of intensification in its final 24 hours prior to landfall in the continental United States are tied with Hurricanes Michael (2018) and Charley (2020) for the second highest in the last two decades, trailing only Zeta, which intensified by 45 kt in the 24 hours before its landfall in Louisiana in late October 2020.